



1
2
3
4
5
6
7
8
9
10
11
12
13
14
15
16
17
18
19
20
21
22
23
24
25
26
27
28
29
30
31
32
33
34
35
36
37
38
39
40
41

Regional scenarios of change over Canada: future climate projections

Zilefac Elvis Asong^{1,2}, Mohamed Elshamy¹, Daniel Princz^{1,3}, Howard Wheeler¹, John Pomeroy^{2,1}, Alain Pietroniro^{1,2,3}, and Alex Cannon⁴

¹Global Institute for Water Security, University of Saskatchewan, 11 Innovation Blvd, Saskatoon, SK, Canada S7N 3H5

²Centre for Hydrology, University of Saskatchewan, 121 Research Drive, Saskatoon, SK, Canada S7N 3C8

³Environment and Climate Change Canada, 11 Innovation Blvd, Saskatoon, SK, Canada S7N 3H5

⁴Climate Research Division, Environment and Climate Change Canada, BC V8W 2Y2, Victoria, Canada

***Corresponding author:**

Phone: +1 306 491 9565

Email: elvis.asong@usask.ca



42 **Abstract**

43 This analysis documents projected changes in daily precipitation and temperature characteristics over
44 Canada based on a 15-member ensemble which had been downscaled using the Canadian Regional
45 Climate Model—CanRCM4 at 50 km resolution by the Canadian Centre for Climate Modelling and Analysis
46 (CCCma) under Representative Concentration Pathway (RCP) 8.5. In this study, the historical CanRCM4
47 simulations are first compared against observations for validation purposes. Then, a multivariate bias
48 correction algorithm is applied to the CanRCM4 outputs to adjust the data against the EU WATCH Forcing
49 Data ERA-Interim reanalysis (WFDEI). We analyze changes in mean and extremes for two 30-year non-
50 overlapping future periods: 2021–2050 and 2071–2100 relative to 1979–2008. The results indicate that
51 daily mean precipitation is projected to increase over Canada, with larger increases expected in the 2080s.
52 However, decreases are projected in summer precipitation over the Canadian Prairies by the year 2100.
53 Mean air temperature is projected to intensify towards the northern high latitude regions, particularly in
54 the winter season. Precipitation and temperature extreme events may increase more than the mean. By
55 examining the behavior of precipitation distribution tails, the mean of the probability distributions of wet
56 extremes over the Saskatchewan (SRB) and Mackenzie River basins (MRB) is projected to shift to the right
57 with global warming. For temperature extremes, minimum temperature may warm faster compared to
58 daily maximum temperatures, particularly in the winter and towards the Arctic region.

59 **Keywords:** Canada; climate projections; precipitation; temperature; extremes

60
61
62
63
64
65
66
67
68
69
70



71 **1 Introduction**

72 Findings of the Intergovernmental Panel on Climate Change (IPCC) Fifth Assessment Report (IPCC,
73 2013) as well as the IPCC Special Report on Global Warming of 1.5°C (Huppmann et al., 2018) demonstrate
74 that increases in anthropogenic greenhouse gases (GHGs) are accelerating the rate of global warming.
75 Associated with a warmer climate are changes over space and time in the characteristics of extreme
76 events such as floods and droughts (Sillmann et al., 2013a;Kharin et al., 2013;Betts et al., 2018). Given the
77 social, economic and ecosystem impacts of these extremes, it is important to provide scale-relevant
78 projections of expected changes in the behavior of these events in order to identify and formulate suitable
79 strategies for water resources systems adaptation and risk management (Kundzewicz et al., 2017;Wilby
80 and Dessai, 2010;Wilby, 2017;IPCC, 2013).

81 The water cycle is closely linked to the climate system. Small, sometimes insignificant variations in
82 climate often lead to significant changes in hydrological processes. In particular, water resources in cold
83 regions are stored mostly in the form of snowpacks and glaciers and have been found to be sensitive to
84 small changes in air temperature. For example, most of the flows in western Canadian rivers rely on
85 headwater supplies from the Rocky Mountains, which make up an important part of the regional and
86 global hydrologic cycle (Pomeroy et al., 2016;Pederson et al., 2011). Given that these high elevation
87 regions are also characterized by a cold region hydro-climate which is seasonally dependent, many
88 existing studies suggest that climate variability and change would be most pronounced in these snow-
89 dominated regions with negative consequences on seasonal and long-term water supplies anticipated
90 (Stocker et al., 2013;Demaria et al., 2016;Islam et al., 2017).

91 Ongoing science hints at the intensification of the hydrologic cycle given the past warming trends
92 which have resulted in significant changes in the hydrological regimes of many North American river
93 basins (DeBeer et al., 2016;Coopersmith et al., 2014;Dumanski et al., 2015;Das et al., 2009). Observational
94 records already indicate that a shift in stream hydrographs (Burn, 1994), and in extreme temperature and



95 precipitation regimes (Vincent et al., 2015;Asong et al., 2016b) have occurred. For the cryosphere,
96 changes in snow and ice regimes—reducing snow cover extent, glacier retreat, thawing of permafrost,
97 and earlier breakup of seasonal freshwater ice cover are occurring as the warming trend continues (IPCC,
98 2013;Woo and Pomeroy, 2011;Woo et al., 1992). Enhanced warming is projected to alter the proportion
99 of precipitation falling in the form of snow and rain, with a declining proportion arriving in the form of
100 snow. Snow pack levels are also expected to form later in the winter, accumulate in smaller quantities,
101 and melt earlier in the season, leading to reduced summer flows (Musselman et al., 2018). The greatest
102 deficits are expected to occur in the summer, thus, decreased soil moisture levels and more frequent and
103 severe droughts are anticipated (Mann and Gleick, 2015;Gleick, 2014;Allen et al., 2010;Arnell, 2008;Li et
104 al., 2009).

105 The foregoing indicates that water resources in cold regions, already stressed with the hazards of
106 natural variability will likely face additional challenges under uncertain climate futures (Arnell, 1999;Bates
107 et al., 2008). At the moment, climate projections are provided by Earth System Models (ESMs), potentially
108 downscaled further with Regional Climate Models (RCMs). However, ESM outputs still cannot be directly
109 applied at the local scale for impacts assessment due to their coarse horizontal resolution (Asong et al.,
110 2016b;Maraun et al., 2017;Maraun et al., 2010). Although subject to many biases, climate change
111 projections offer a glimpse into possible future water resource impacts and challenges. To reduce biases
112 and overcome the scale mismatch between the ESM/RCM outputs and the desired scale for impact
113 assessment, climate model outputs are often bias-corrected to historical observations (Maraun et al.,
114 2017;Cannon, 2016;Volosciuk et al., 2017).

115 The goal of the current study, therefore, is to analyze future changes in precipitation and
116 temperature characteristics over Canada. These are key variables which govern hydrological cycle
117 dynamics and are of paramount importance to hydrological processes in a changing climate. To this end,
118 a 15-member ensemble under Representative Concentration Pathway (RCP) 8.5, downscaled by the



119 Canadian Centre for Climate Modelling and Analysis (CCCma) as part of the Canadian Sea Ice and Snow
120 Evolution Network (CanSISE) Climate Change and Atmospheric Research (CCAR) Network project, is
121 utilized in this study. As mentioned above, these outputs often contain biases, thus, a multivariate
122 quantile mapping approach is first applied to bias-correct the climate model simulations against the
123 European Union Integrated Project Water and Global Change (WATCH) ERA-Interim reanalysis (WFDEI) at
124 $3\text{h} \times 0.5^\circ$ resolution. We investigate further the consequences on the projected climate change signals of
125 applying bias correction to the raw climate model outputs.

126 The paper is organized as follows. The study area and data are described in section 2. In section 3,
127 we provide the methodology for bias correction, calculation of climate indices, and how projected climate
128 signals are computed both for the mean and extreme states. The results and discussion are presented in
129 section 4 and 5, respectively, while a summary of the main findings and conclusions are presented in
130 section 6.

131 **2 Study area and data sets**

132 **2.1 Study area**

133 The case study (Fig. 1) includes the Canada continental domain south of latitude 72° N. This region
134 contains major river basins such as the Great Lakes and St. Lawrence River systems, which is one of the
135 largest freshwater resources in North America and globally. This region also comprises two main natural
136 systems—the Saskatchewan (SRB) and Mackenzie River basins (MRB) which are testbeds for the Changing
137 Cold Regions Network—CCRN (<http://www.ccrnetwork.ca/> , last access: 6 March 2019) large-scale
138 hydrological modelling strategy. The Prairies of Canada are characterized by a highly varying climate and
139 decreasing water resources. This region is also prone to droughts such those in 1988 and 1999–2005
140 (Asong et al., 2018), as well as damaging floods in 2011, 2013, and 2014 (Burn and Whitfield, 2017; Burn
141 et al., 2016).



142 **2.2 Gridded observations**

143 In order to bias-correct the climate model outputs, gridded sub-daily retrospective meteorology
144 that describe well the historical climate over Canada are required. Several gridded products exist over this
145 region, including the Princeton (Sheffield et al., 2006), the North American Regional Reanalysis (Mesinger
146 et al., 2006), WFDEI (Weedon et al., 2014), forecasts of the Global Environmental Multiscale(GEM)
147 atmospheric model (Yeh et al., 2002), and the Canadian Precipitation Analysis—CaPA (Mahfouf et al.,
148 2007) data sets. Wong et al. (2017) performed an inter-comparison of precipitation estimates from these
149 products against observed station data over Canada. They found the CaPA and WFDEI products to have
150 close agreement with station observations. Nevertheless, GEM-CaPA which is available for the period 2004
151 – 2016 is not only too short for bias-correcting ESM climate, variables such as air temperature and specific
152 humidity are issued at 40 m height (projected changes in temperature are often analyzed at 2 m height
153 since this is the level that is most relevant to biophysical and human activities).

154 The WFDEI variables such as air temperature and specific humidity are issued at the surface and a
155 comparative analysis against ground measurements shows that it outperforms other products in Canada
156 and the United States (Chadburn et al., 2015;Wong et al., 2017;Park et al., 2016;Behnke et al.,
157 2016;Sapiano and Arkin, 2009). Therefore, the 3-h \times 0.5° WFDEI product (1979 – 2016) is used in this
158 study. We utilize the Global Precipitation Climatology Centre product (GPCC) version of WFDEI (WFDEI-
159 GPCC) data set which has improved precipitation estimates relative to the Climate Research Unit (CRU)
160 based product—WFDEI-CRU (Weedon et al., 2014) when compared against ground observations in our
161 domain of interest.

162 **2.3 Regional climate model outputs**

163 The climate projections utilized in this study are sourced from the Canadian Centre for Climate
164 Modelling and Analysis (CCCma) and are available at www.cccma.ec.gc.ca/data/canrcm/CanRCM4 (last
165 access: 6 March 2019). The simulations span the North American domain defined by the Coordinated



166 Regional Climate Downscaling Experiment for North America (CORDEX) project
167 (<http://www.cordex.org/domains/region1-north-america/>, last access: 24 April 2019) from 1950-2100.
168 Scinocca et al. (2016) downscaled outputs from the Second Generation Canadian Earth System Model
169 (CanESM2), using a new RCM, the CCCma Regional Climate Model (CanRCM4) under RCP4.5 and RCP8.5.
170 The forcing data for the historical runs (1950 – 2005), and future (2006 – 2100) simulations of CanRCM4
171 are derived from CanESM2 following the Coupled Model Intercomparison Project Phase 5 (CMIP5)
172 protocols. The CanRCM4 large ensemble which consists of 50 members were downscaled at 0.44° (50 km)
173 and 0.22° (25 km) horizontal resolutions. This large ensemble is an extension of the CanESM2 simulations
174 proposed by the Canadian Sea Ice and Snow Evolution Network (CanSISE) Climate Change and
175 Atmospheric Research (CCAR) Network project (<https://www.cansise.ca/>, last access: 24 April 2019). For
176 this study, we used 15 members of the 0.44 degrees resolution product at 1-h time step under RCP8.5.
177 The choice of number of ensembles examined is based solely on public data availability at the time of this
178 analysis. The seven climate variables required for driving the CCRN hydrological models and which are
179 bias corrected in this study are listed in Table 1. Nonetheless, only projected changes in precipitation and
180 air temperature are analyzed in this paper.

181 **3 Methodology**

182 **3.1 Data processing and multivariate bias correction**

183 In order to bias correct CanRCM4 outputs against WFDEI, both data sets must have the same
184 temporal and spatial dimensions. Prior to bias-correction, the 1-h CanRCM4 estimates were aggregated
185 to 3-h values for consistency with the WFDEI data. CanRCM4 was further re-gridded to match the WFDEI
186 specifications using nearest neighbor interpolation as implemented in the Climate Data Operators
187 software (<https://code.mpimet.mpg.de/projects/cdo/>, last access: 23 November 2018). For bias
188 correction which accounts for dependence between the different variables (Table 1), an image processing
189 technique described in Cannon (2018) for multivariate bias correction (MBCn) of climate model outputs



190 was utilized. Models are fitted to data for each calendar month across each pixel in the study area while
191 preserving the dependence structure among variables. The historical data sets used in the fitting
192 procedure include WFDEI (1979 – 2008) and CanRCM4 (1979 – 2008). Using the fitted models, we apply
193 changes in quantiles to CanRCM4 output from 1950 – 2100.

194 **3.2 Assessing changes in mean climate**

195 In order to evaluate the projected climate change signals with respect to the reference period
196 (1979–2008), two 30-year time windows (2021–2050 and 2071–2100) are studied. Using the 15-member
197 ensemble, the climate change signal is investigated in terms of both the mean and extremes of
198 precipitation and temperature. To investigate changes in mean climate, mean daily precipitation and
199 temperature are computed for each ensemble member, and delta statistics are derived between the
200 historical and future periods (delta statistics converted to relative percentage changes in the case of
201 precipitation). The changes are derived for the time periods mentioned above: 2021–2050 (2030s) and
202 2071–2100 (2080s) with respect to 1979–2008 (1990s). The projected changes are computed by season:
203 summer (JJA), autumn (SON), winter (DJF), and spring (MAM).

204 **3.3 Assessing changes in climate extremes**

205 Investigations of future changes in temperature and precipitation extremes have focused
206 primarily on two approaches. The first is based on indices of climate extremes with return periods of
207 about a year or less (e.g. extremely wet days, diurnal temperature range). The second method focuses
208 on extreme value theory which is important for assessing the vulnerability of engineering infrastructure
209 to climate change (Kharin et al., 2007; Asong et al., 2015; Coles et al., 2001). While climate extremes in a
210 in a climate change context are often studied in these two ways, this study investigates changes in climate
211 extremes using the first method which has a much broader context and can be useful for investigating the
212 hydrologic and water resource implications of climate change (Sillmann et al., 2013b). A set of 27 indices
213 focusing mainly on climate extremes has been made available by the Expert Team on Climate Change



214 Detection and Indices—ETCCDI (http://etccdi.pacificclimate.org/list_27_indices.shtml , last access:
215 6 March 2019) (Karl et al., 1993;Karl and Easterling, 1999;Zhang et al., 2011). In the present study, the
216 ETCCDI indices were computed as implemented in the Pacific Climate Impacts Consortium’s
217 “*climdex.psic.ncdf*” package (<http://pacificclimate.github.io/climdex.psic.ncdf/>, last access:
218 6 March 2019). The default thresholds prescribed in the package for computing these indices are used
219 here. Where applicable, changes in the indices over the 2030s and 2080s are analyzed relative to the
220 1990s (see section 3.2 for details). The following water resource-relevant indices are further examined in
221 this study: maximum 5–day Precipitation (RX5day); maximum 1–day Precipitation (RX1day); extremely
222 wet days (R99p); monthly minimum value of daily minimum temperature (TNn); monthly maximum value
223 of daily maximum temperature (TXx); and diurnal temperature range (DTR). Details on these indices are
224 found in Sillmann et al. (2013b), Sillmann et al. (2013a), on the ETCCDI website as well as in the
225 *climdex.psic.ncdf* package manual.

226 **4 Results**

227 This section presents the results and a discussion of various analyses described in section 3.
228 Assessment of CanRCM4 outputs against WFDEI and the performance of the MBCn algorithm is shown
229 first followed by future changes in mean and extremes of precipitation and temperature. Raw CanRCM4
230 (CanRCM4_Raw) outputs are also discussed to assess the skill of MBCn in preserving the simulated climate
231 change signals. We present the results in two dimensions: (1) temporal plots of areal averaged
232 characteristics over the MRB and SRB for RCP8.5 from 1950 – 2100, (2) spatial patterns of simulated
233 changes for the 2030s and 2080s, and (3) probability distributions that reveal the tail characteristics of
234 seasonal precipitation indices over the MRB and SRB. For spatial changes, results are shown for the 15-
235 member ensemble mean. Emphasis is placed on the unbiased (CanRCM4_Corr) CanRCM4 simulations
236 while the impact of bias correction on the results is discussed in section 4.4 for both CanRCM4_Corr and
237 CanRCM4_Raw.



238 4.1 Evaluation and bias correction of climate variables

239 RCM outputs are known to contain biases that are mostly inherited from the driving ESM (Ehret
240 et al., 2012; Laprise, 2008). Thus, we begin our analysis by showing why there is the need to bias-correct
241 CanRCM4 output. For this purpose, threshold exceedance indices such as the days with precipitation > 1
242 mm (R1mm), and consecutive dry (CDD) and wet days (CWD) are computed from both WFDEI and 15
243 members of the CanRCM4 outputs (precipitation threshold = 1 mm) during 1979 – 2008. Figure 2a shows
244 quantile-quantile plots of R1mm for the study domain. It is evident that CanRCM4 tends to underestimate
245 the number of wet days. Concerning CDD and CWD averaged across longitudinal bands for the entire
246 study domain, CanRCM4 overestimates CWD (Fig. S1a). However, CanRCM4 agrees well with WFDEI in
247 terms of CDD except from latitude 60° poleward where CDD is underestimated by CanRCM4. It is worth
248 mentioning that the performance of WFDEI north of 60° N is questionable given the paucity of observed
249 meteorological data in these high latitude environments (Weedon et al., 2014; Beck et al., 2017).

250 Next, we assess whether the bias is removed after applying MBCn to the raw 3-h CanRCM4
251 outputs. Figure 2b depicts quantile-quantile plots of R1mm after bias correction. The MBCn algorithm
252 shifts the distribution of CanRCM4 to match that of WFDEI although the number of wet days are slightly
253 underestimated by MBCn. Note that R1mm is a derived quantity from the 3-h data (bias correction was
254 performed at the 3-h resolution). The impact of bias correction on the wet-dry day physics produced by
255 the climate model can be substantial and have been recognized as one of the reasons why bias correction
256 should be applied with care (Ehret et al., 2012; Johnson and Sharma, 2012). Figure S2 shows the spatial
257 patterns of 3-h precipitation averaged over the reference period (1979 – 2008) for the uncorrected
258 (CanRCM4_Raw) and corrected (CanRCM4_Corr) simulations as well as the mean bias (CanRCM4_Corr –
259 WFDEI). As shown in Fig. S2, the spatial patterns of precipitation between CanRCM4_Raw and
260 CanRCM4_Corr are very similar since biases are corrected per grid point. The bias (CanRCM4_Corr –
261 WFDEI) is very close to zero across the study domain, implying that MBCn was able to correct the statistical



262 properties of CanRCM4 simulated precipitation amounts to match those of WFDEI. The same holds true
263 in the case of air temperature (Fig. S3). This discussion is substantiated further in section 4.4.

264 **4.2 Future projections of mean climate**

265 **4.2.1 Projected changes in daily precipitation**

266 We begin this section by presenting results of the temporal evolution and projected spatial
267 patterns of CanRCM4_Raw and CanRCM4_Corr climate. Figure 3 shows the time series of daily
268 precipitation over the MRB and SRB as simulated by the 15-member CanRCM4 ensemble. Both the
269 individual simulations as well the ensemble mean of the 15 realizations are shown. Over the MRB,
270 compared to the historical period, mean precipitation may likely increase by the year 2100. Seasonally,
271 the relative change is 15% (DJF), 15% (MAM), 14% (JJA), and 25% (SON) by the year 2100 based on the
272 mean of 15 ensemble members. For the SRB, apart from a decrease in summer precipitation, the
273 projections indicate that mean precipitation may increase in the future. Seasonally, the relative change is
274 20% (DJF), 19% (MAM), -6% (JJA), and 11% (SON) by the year 2100. In terms of variability, precipitation
275 variability is higher over SRB compared to MRB as shown by the large inter-realization spread. Also, there
276 is no noticeable difference between CanRCM4_Raw and CanRCM4_Corr daily precipitation.

277 Projected changes in the spatial and seasonal patterns of mean precipitation are depicted in Fig.
278 4. It is evident that the changes are seasonally dependent. CanRCM4 projects a likely increase in mean
279 precipitation over most of the study area for all seasons. The increase may be greater in the 2080s
280 compared to the 2030s. In the JJA, a large belt of the Canadian Prairies may expect a decrease in mean
281 precipitation of about 15% by 2100 while eastern and northern regions may experience up to 80% increase
282 in precipitation during the same season. Summaries of possible changes in precipitation over the MRB
283 and SRB are presented in Table 2. Apart from a projected decrease (-1.5%) in mean precipitation during
284 the JJA over SRB in the 2080s, both basins may experience an increase in precipitation in the 2030s and



285 2080s. Larger changes are projected for the SRB compared to the MRB, particularly in the MAM, DJF and
286 SON in the 2080s.

287 **4.2.2 Projected changes in daily mean temperature**

288 The temporal evolution of daily mean temperature averaged over the MRB and SRB as simulated
289 by the 15-member CanRCM4 ensemble is shown in Fig. 5. Both the individual simulations as well the
290 ensemble mean of the 15 realizations are shown. Over the MRB, compared to the historical period, mean
291 temperature may increase by the end of the 21st century. Seasonally, an increase in air temperature of
292 ~2.5°C by the year 2100 based on the mean of 15 ensemble members is projected for all seasons and river
293 basins. The projections further indicate not only warming conditions, but air temperature in DJF and MAM
294 will likely be more variable compared to JJA and SON.

295 For mean air temperature (Fig. 6), relative to the 1990s, a projected increase on seasonal and
296 annual time scales over the study area is expected for the future periods. The warming will likely intensify
297 in the 2080s compared to the 2030s. Spatially, most of the warming will probably occur over the artic
298 region where mean temperature of ~10°C is projected by 2100. Seasonally, higher warming is simulated
299 for the DJF season both in the 2030s and 2080s. Although mean temperature is projected to increase for
300 the whole domain in JJA, most of the warming will likely concentrate on the Prairies, over the Rocky
301 Mountains, and most of southern British Columbia in the 2080s. Table 3 summarizes changes in mean
302 temperature for the MRB and SRB. The DJF season may experience the most warming of about 8.6°C over
303 the MRB during the 2080s. However, the case is different for the SRB where the most warming of 7.2°C is
304 projected in the JJA during the 2080s. In general, larger changes in temperature are projected for other
305 seasons (apart from JJA) over the MRB compared to the SRB. The MRB is a located north of the SRB, thus
306 the south-north spatial warming trend projected for the whole domain corroborates this finding.



307 **4.3 Future projections of climate extremes**

308 **4.3.1 Precipitation extremes**

309 Projected changes in selected precipitation indices (RX5day, R99p, and RX1day) are presented
310 here. Changes in the spatial patterns of maximum 5-day precipitation (RX5day) are illustrated in Fig. 7. As
311 expected, the spatial structure of changes in RX5day is similar to that of mean precipitation (Fig. 4).
312 Relative to the 1990s, CanRCM4 projects an increase (>100%) in RX5day over most of Canada in DJF, MAM,
313 JJA, and SON, with higher increases in the 2080s compared to the 2030s. Using the 2080s as an example,
314 increases in RX5day may be greater in DJF over most of the Prairies and the Arctic region. However, in JJA,
315 the spatial patterns of changes are different compared to DJF. Decreases in RX5day of about -30% are
316 projected for the Prairies in JJA in the 2080s. On a river basin scale, summaries of projected changes in
317 RX5day over the MRB and SRB are presented in Table 4 for all four seasons. Over the MRB (SRB), RX5day
318 is projected to increase by 30.6 (46.7) %, 45.5 (52.6) %, and 39.5 (32.3) % in DJF, MAM, and SON,
319 respectively, by the year 2100. However, in JJA, RX5day is projected to increase by 15.6% over the MRB
320 while a decrease of -1.7% is projected for the SRB in the 2080s.

321 Figure 8 displays changes in extremely wet days (R99p) during the 2030s and 2080s. Compared to
322 the historical period, R99p is projected to almost double (~180%) by the 2080s. Spatially, increases of up
323 to 140% are projected over the eastern and western parts of Canada by 2100. However, patches of small
324 (<15%) or no change (0%) in R99p are projected for the southern and central regions (e.g. the Prairies) of
325 the study domain. Furthermore, changes in the characteristics of precipitation extremes in a future
326 climate were examined by plotting the probability distributions (PDFs) of seasonal maximum 1-day
327 precipitation (RX1day) averaged over the MRB and SRB (Fig. 9). For the PDFs, across the MRB and SRB,
328 larger tails are projected for the JJA compared to other seasons, and more so for the 2080s. RX1day is
329 projected to shift (i.e. change in the mean) to the right with global warming (Table S1). In the MRB, relative
330 to the 1990s, changes in the mean of RX1day in the 2030s (2080s) are 14.3 (32.6%), 15.5 (42.2%), 7.4



331 (12.8%), and 16.3 (43.0%) for DJF, MAM, JJA, and SON, respectively. Similarly, for the SRB, mean changes
332 for RX1day in the 2030s (2080s) are 16.9 (47.2%), 20.2 (48.9%), 2.4 (-5.4%), and 17.0 (34.0%) for DJF,
333 MAM, JJA, and SON, respectively.

334 4.3.2 Temperature extremes

335 Temperature extremes are examined here in terms of spatial and seasonal patterns of TNn, TXx
336 and DTR. The projected mean changes of TNn, TXx and DTR as simulated by the CanRCM4 15-member
337 ensemble are shown in Fig. 10 for the 2080s. Noticeably, TNn (Fig. 10a) increases more than TXx (Fig. 10b).
338 Also, TNn and TXx show dissimilar spatial and seasonal patterns. TNn shows clear distinct spatial and
339 seasonal patterns compared to TXx. Particularly, TNn amplifies in the northern regions than in the
340 southern latitudes. Seasonally, changes in TNn of more than 15°C are projected for the DJF season across
341 much of Canada. The least changes (<3°C) in TNn are projected for the warm season (JJA).

342 Apart from TNn and TXx, changes in the DTR were analyzed since DTR is a useful index of global
343 climate change. Using observational records, it has been found that DTR has decreased significantly since
344 the year 1950 because of differential changes in minimum and maximum temperatures. There is much
345 debate surrounding the evaluation of DTR in current observational datasets and the capabilities of ESMs
346 to represent its characteristics in a future climate (Thorne et al., 2016; You et al., 2017; Lewis and Karoly,
347 2013; Braganza et al., 2004). Figure 10c shows changes in DTR in the 2080s relative to the 1990s. There is
348 a projected decrease (up to -3°C) in DTR in the DJF and MAM seasons for most of Canada. In the JJA, DTR
349 is projected to increase (~2.5°C) over much of western Canada. In the SON and on an annual scale (ANN),
350 DTR is projected to decrease more uniformly over the study area.

351 Basin-scale summaries of changes in TNn, TXx and DTR over the MRB and SRB for the 2080s are
352 shown in Table 5. In the MRB, relative to the 1990s, the largest (smallest) projected increase in TNn of
353 9.4°C (6.1°C) is in DJF (JJA). For TXx, the largest (smallest) increase 6.2°C (3.3°C) is in JJA (MAM). For DTR,
354 decreases are projected for DJF (-1.2°C), MAM (-1.4°C) and SON (-0.8°C), while an increase is projected for



355 the JJA (0.1°C). Similarly, In the SRB, relative to the 1990s, the largest (smallest) projected increase in TNn
356 of 9.3°C (6.1°C) is in DJF (MAM). For TXx, the largest (smallest) increase 7.2°C (2.7°C) is in JJA (DJF). And
357 for DTR, decreases are projected for DJF (-1.9°C), MAM (-1.1°C) and SON (-0.5°C), while an increase is
358 projected for the JJA (0.4°C). In both basins, the change in TNn (TXx) is greater in DJF (JJA) compared to
359 other seasons. This in turn explains the projected decrease (increase) in DTR during these seasons.

360 **4.4 Impact of bias correction on the simulated climate change signals**

361 This section discusses the impact that bias correction has on the CanRCM4_Raw outputs. Whether
362 bias correction should be applied to climate model outputs remains a contentious issue in the climate
363 change impacts community for many reasons (Ehret et al., 2012). Also, raw climate model outputs include
364 systematic biases that affect the climate change signals of high-impact meteorological fields such as
365 precipitation and temperature. Throughout the paper, we have shown results for both CanRCM4_Raw
366 and CanRCM4_Corr. Here, we investigate whether the simulated climate change signal was preserved
367 after applying MBCn to the CanRCM4_Raw outputs. The temporal plots in Figs. 3 and 5 clearly indicate
368 that MBCn can preserve precisely the inter-annual variability of precipitation and temperature as
369 simulated by the CanRCM4. Fig. 11 shows the impact of bias correction on the seasonal cycle of daily mean
370 precipitation and temperature over the MRB and SRB. Firstly, there is a large wet bias in CanRCM4_Raw
371 precipitation particularly in MAM, JJA and SON, and a warm bias in temperature, particularly during winter
372 (DJF) relative to WFDEI averaged over the MRB and SRB. This also necessitated the application of MBCn
373 on the raw CanRCM4 outputs. By comparing the CanRCM4 historical (1990s) simulations against WFDEI,
374 it is clear that MBCn removes satisfactorily the bias in the CanRCM4_Raw outputs.

375 On the projected climate signal, there is both a projected change in the amplitude of precipitation
376 as well as a shift in the phase of the cycle over the MRB with global warming. In the 1990s and 2030s,
377 peak precipitation occurs in July, however, by the 2080s, the precipitation peak is projected to occur in
378 June. Although CanRCM4 projects wetter conditions in a warmer climate for the SRB, no noticeable



379 change in the phase of the cycle with global warming is anticipated. This is also true for the annual cycle
380 of mean temperature over MRB and SRB where warmer air temperatures are projected throughout the
381 year by 2100. These climate change signals are very well preserved after applying MBCn to the
382 CanRCM4_Raw outputs. It is worth stating that future research needs are on developing process-based
383 bias correction methods that depend on simulated intensities rather than preserving the raw climate
384 change signal from climate models (Ivanov et al., 2018;Maraun et al., 2017).

385 **5 Discussion**

386 The foregoing analyses have indicated that mean precipitation and temperature will likely
387 increase over Canada, especially by the end of the 21st century. Nevertheless, the projected changes are
388 seasonally and regionally dependent. For example, over the SRB (MRB), a decrease (increase) in mean
389 precipitation is projected in the JJA by the year 2100. Regarding spatial patterns of warming, there is a
390 general south-north heating trend with the polar (arctic) regions projected to warm the most under
391 RCP8.5. With regard to wet and warm extremes, the derived climate indices will probably increase more
392 than the mean. Another interesting dynamic is that regions affected by smaller changes in the mean also
393 tend to have the smallest projected changes in the magnitude of extremes, and vice versa. The SRB is
394 projected to get drier in the JJA, accompanied with a decrease in wet extremes. However, mean and
395 extreme temperature are projected to likely increase over this basin. This points to a possible
396 intensification of meteorological drought over this river basin in a warmer climate.

397 By comparing the bias-corrected (CanRCM4_Corr) climate signals against the raw outputs
398 (CanRCM4_Raw), CanRCM4_Raw overestimates the amplitude of the seasonal cycle of projected
399 precipitation and temperature (Fig. 11) although temperature well reproduced compared to precipitation.
400 The comparison does not only aid in assessing the skill of the CanRCM4 in reproducing observed historical
401 climate but also illustrates the need for bias-correcting CanRCM4 outputs against WFDEI. Whether or not
402 bias correction algorithms should be applied to ESM outputs is a subject of much debate. However,



403 systematic biases (as highlighted above) and fitness for purpose, such as the need to drive cold regions
404 hydrologic models which require high resolution inputs (Willkofer et al., 2018; Wood et al., 2004)
405 necessitated the current exercise. As mentioned previously, the results discussed here are based on
406 outputs from one RCM. However, the CMIP5 ensemble has a large spread and conclusions based on one
407 climate model should be interpreted with caution.

408 The results discussed in this study are certainly in line with existing literature. For projected
409 changes in mean climate, the IPCC AR5 findings indicate that “high latitudes are *very likely* to experience
410 greater amounts of precipitation due to the increased specific humidity of the warmer troposphere as
411 well as increased transport of water vapor from the tropics by the end of this century under the RCP8.5
412 scenario.” Kharin et al. (2007) and Sillmann et al. (2013a) found a probable increase in precipitation and
413 temperature extremes over North America using a multi-model ensemble approach. Nevertheless, the
414 above studies were done on annual scales. But, our findings using downscaled CanESM2 outputs agree
415 (regarding the direction of change) with such previous analyses which investigated future changes in
416 precipitation and temperature characteristics at coarse scale.

417 At the regional scale, several studies have been carried out using RCMs which still operate at
418 horizontal resolutions larger than 20 km to investigate future changes in climate over Canada. For
419 example, Wang et al. (2015) used the PRECIS RCM to generate a large ensemble climate simulations over
420 Ontario, Canada, between 1950 to 2099, forced at the boundary by perturbed physics from the HadCM3
421 ensemble under the SRES A1B emissions scenario. They found a tendency towards a warming trend over
422 the study region in the range of 2.6-2.7°C in the 2030s, and 5.9-7.4°C in the 2080s. Similarly, they found
423 an increase in annual total precipitation of 4.5-7.1% during the 2030s and 3.2- 17.5% for the 2080s. In
424 terms of temperature extremes, Jeong et al. (2016) analyzed future changes in hot events over Canada by
425 analyzing eleven RCM outputs from the North American Regional Climate Change Assessment Program
426 (NARCCAP), under the A2 emission scenario. Their results suggested a likely intensification in the



427 frequency of hot days. Nevertheless, the projected changes showed high spatial variability and were
428 highly dependent on the RCM and parent GCM combination. For precipitation extremes, Monette et al.
429 (2012) investigated changes in single- and multi-day events as simulated by six RCMs from the NARCCAP
430 ensemble. They found a projected increase to various return levels for multiple Northeast Canadian
431 watersheds during the future (2041–2070) period relative to the historical (1971–2000) period.

432 An analysis of changes in precipitation and temperature characteristics have also been carried out
433 based upon high-resolution RCM projections at the 10 km scale. Erler et al. (2015) and Erler and Peltier
434 (2016) analyzed changes in climate extremes in western Canada based upon an ensemble of high-
435 resolution regional climate projections dynamically downscaled to 10 km resolution with the aid of the
436 Weather Research and Forecasting (WRF) model in two different configurations with convection
437 parameterized in the model. The simulations were performed for three 15-yr periods: a historical period
438 from 1979 – 1994, a midcentury period from 2045 – 2060, and an end-century period from 2085 – 2100
439 under RCP 8.5. They found that changes in wet extremes generally followed projected changes in the
440 mean, although the likely changes in mean and extreme precipitation differed strongly across seasons and
441 regions. Furthermore, the projections showed an increase in DJF precipitation during the 2050s, whereas
442 net precipitation in summer is projected to decrease as a result of increased evapotranspiration.

443 Generally, irrespective of horizontal resolution, previous studies agree in terms of the trend in air
444 temperature with global warming. Although coarse resolution models (e.g. GCMs) project an increase in
445 seasonal precipitation over Canada, the 10 km WRF simulations discussed above indicate a potential
446 decrease in JJA precipitation over western Canada. However, wet extremes are projected to intensity at
447 the same time albeit the CanRCM4 ensemble investigated here indicate a likely decrease in maximum 5-
448 day precipitation (RX5day) in JJA over the Canadian Prairies.



449 **6 Summary and conclusions**

450 Future changes in daily precipitation and temperature characteristics over Canada are
451 documented in this study as part of the Changing Cold Regions Network (CCRN) future scenarios of change
452 initiative. For this purpose, relevant climate variables were obtained from CCCma. Outputs from CanESM2
453 have been downscaled dynamically by using the CCCma Regional Climate Model (CanRCM4) at 0.44° (50
454 km) horizontal resolution under RCP8.5. After evaluating the CanRCM4 data against observations,
455 substantial biases were found. Therefore, a multivariate bias correction algorithm was applied to the
456 climate model outputs to adjust the data against a gridded climate product (WFDEI). Subsequently, we
457 investigated whether the raw climate change signals were preserved after applying bias correction to the
458 original data. Changes in mean climate and extremes are computed for two 30-year non-overlapping
459 future periods: 2021–2050 (2030s) and 2071–2100 (2080s) relative to 1979–2008 (1990s), and for four
460 seasons: DJF, MAM, JJA and SON as well as on an annual (ANN) basis. Based on these analyses, the most
461 important findings of our study include:

462 (1) In terms of the temporal evolution, mean precipitation may increase over the MRB by the end of the
463 21st century. On a seasonal basis, higher increases are projected for the SON, DJF, MAM, and JJA,
464 respectively. Over the SRB, apart from a likely decrease in JJA precipitation, increases in mean
465 precipitation are projected for DJF, MAM and SON, respectively by the year 2100. Spatially, the
466 projections indicate an increase in precipitation over most of Canada, with larger increases expected
467 in the 2080s. However, decreases are projected for the southwestern parts of the United States in the
468 DJF and MAM. In the JJA, a large belt of the Canadian Prairies may expect a decrease in mean
469 precipitation by the end of the 21st century. Apart from a projected decrease in precipitation for the
470 JJA over the SRB, both basins may experience an increase in precipitation in the 2030s and 2080s.

471 (2) Relative to the historical period, mean air temperature over Canada is projected to intensify with
472 increasing radiative forcing in the future. Temporally, the areal averaged time series over MRB and



473 SRB indicate that air temperature in DJF and MAM will likely be more variable compared to JJA and
474 SON. The spatial patterns of changes in mean temperature show strong increases in the northern high
475 latitude regions, particularly in the DJF season. On a river basin scale, the DJF season may experience
476 the most warming of about 8.6°C over the MRB during the 2080s. However, the case is different for
477 the SRB where the most warming of 7.2°C is projected in the JJA during the 2080s.

478 (3) Regarding wet and warm extremes, the examined climate indices are projected to increase more than
479 the mean over the study area by the end of the 21st century. In terms of the probability distribution
480 of extremes, across the MRB and SRB, larger tails are projected for the JJA compared to other seasons,
481 and more so for the 2080s. For temperature extremes, T_N is projected to warm faster than T_X,
482 particularly in the DJF and towards the poles. This in turn results in a projected decrease in DTR,
483 implying that warmer air temperatures may prevail throughout the year in a warmer climate. Also,
484 regions affected by smaller changes in the mean also tend to experience the smallest projected
485 changes in the magnitude of extremes, and vice versa. The SRB is projected to get drier in the JJA,
486 accompanied with a decrease in wet extremes. However, mean and extreme temperature are
487 projected to likely increase over this basin.

488 (4) Compared to observations, the raw CanRCM4 outputs contained systematic biases which
489 necessitated bias correction towards WFDEI. Throughout the paper, the impact of the climate change
490 signal based on the uncorrected and corrected data have been discussed. We found a large difference
491 between the climate indices computed from both data sets. For example, in Fig. 11, the climatological
492 daily mean temperature over the MRB in July for CanRCM4_Raw in the 1990s is 18°C while the
493 corrected one is ~13 °C. This results in a 5 °C warm bias which can have various consequences for
494 hydrology and water resources management. Therefore, it was of paramount importance to evaluate
495 CanRCM4 outputs for the presence of biases and correcting these outputs towards WFDEI prior to



496 deriving the projected climate change signals shown here. Nonetheless, the WFDEI product is not
497 perfect and caution should be exercised when interpreting these results.

498 (5) Finally, it is worth mentioning that the results presented in this study are in line with findings from
499 the IPCC AR5. Furthermore, the analyses utilized outputs from only one global climate model
500 (CanESM2) and one RCM (CanRCM4), however, there exist a large spread in the CMIP5 multi-model
501 ensemble. This limitation can be overcome in future studies by evaluating additional RCM outputs
502 from the CORDEX-NA larger ensemble. It is hoped that such efforts will strengthen further the findings
503 of this study. While we did not explain the physical basis for the projected changes of precipitation
504 and temperature documented here, it is recommended that future changes in temperature and
505 precipitation characteristics be evaluated in relation to changes in atmospheric circulation patterns,
506 and feedback mechanisms such as snow cover changes, soil moisture, and vegetation dynamics.

507 **Competing interests**

508 The authors declare that they have no conflict of interest.

509 **Special issue statement**

510 This article is part of the special issue “Understanding and predicting Earth system and hydrological
511 change in cold regions”. It is not associated with a conference.

512 **Acknowledgements**

513 We acknowledge the World Climate Research Programme's Working Group on Coupled Modelling, which
514 is responsible for CMIP, and we thank the climate modeling groups for producing and making available
515 their model output. For CMIP the U.S. Department of Energy's Program for Climate Model Diagnosis and
516 Intercomparison provides coordinating support and led development of software infrastructure in
517 partnership with the Global Organization for Earth System Science Portals. We also thank the Canadian
518 Centre for Climate Modelling and Analysis for making available the CanRCM4 outputs.

519



520 **List of Tables**

521 **Table 1:** List of seven variables used for multivariate bias correction. The heights and units for each
 522 variable are shown

Variable	WFDEI		CanRCM4	
	Height	Unit	Height	Unit
Precipitation	Surface	kg m ⁻² s ⁻¹	Surface	kg m ⁻² s ⁻¹
Air Temperature	2 m	K	2 m	K
Specific Humidity	2 m	kg kg ⁻¹	2 m	kg kg ⁻¹
Wind Speed	10 m	m s ⁻¹	10 m	m s ⁻¹
Surface Pressure	Surface	Pa	Surface	Pa
Surface Downwelling Shortwave Radiation	Surface	W m ⁻²	Surface	W m ⁻²
Surface Downwelling Longwave Radiation	Surface	W m ⁻²	Surface	W m ⁻²

523

524 **Table 2:** Summary of projected changes (%) in daily mean precipitation for DJF, MAM, JJA, SON, and annual
 525 (ANN) scales during the 2021–2050 (2030s) and 2071–2100 (2080s) relative to 1979–2008 (1990s) over
 526 the Mackenzie (MRB) and Saskatchewan (SRB) River basins

	MRB				SRB			
	2030s		2080s		2030s		2080s	
	<i>raw</i>	<i>corr</i>	<i>raw</i>	<i>corr</i>	<i>raw</i>	<i>corr</i>	<i>raw</i>	<i>corr</i>
DJF	12.4	12.0	28.8	26.7	15.7	15.4	48.0	46.6
MAM	17.1	17.5	49.8	47.9	19.9	23.2	51.2	56.7
JJA	9.4	9.7	18.1	18.8	1.9	2.5	-1.8	-1.5
SON	17.0	18.1	41.9	42.9	18.2	20.7	38.8	42.9
ANN	12.9	13.7	30.5	31.7	10.3	12.8	22.5	27.9

527

528

529

530

531

532

533



534 **Table 3:** Summary of projected changes (°C) in daily mean temperature. Other information is the same as
 535 in Table 2.

	MRB				SRB			
	2030s		2080s		2030s		2080s	
	<i>raw</i>	<i>corr</i>	<i>raw</i>	<i>corr</i>	<i>raw</i>	<i>corr</i>	<i>raw</i>	<i>corr</i>
DJF	3.3	3.3	8.5	8.6	2.6	2.6	6.4	6.4
MAM	1.9	1.9	5.1	5.2	1.5	1.5	4.2	4.2
JJA	2.4	2.4	6.1	6.1	2.8	2.7	7.2	7.2
SON	2.4	2.4	6.3	6.4	2.1	2.0	5.7	5.8
ANN	2.5	2.5	6.6	6.6	2.2	2.2	5.8	5.9

536
 537 **Table 4:** Summary of projected changes (%) in maximum 5-day precipitation (RX5day) for DJF, MAM, JJA,
 538 and SON during the 2021–2050 (2030s) and 2071–2100 (2080s) relative to 1979–2008 (1990s) over the
 539 Mackenzie (MRB) and Saskatchewan (SRB) River basins

	MRB				SRB			
	2030s		2080s		2030s		2080s	
	<i>raw</i>	<i>corr</i>	<i>raw</i>	<i>corr</i>	<i>raw</i>	<i>corr</i>	<i>raw</i>	<i>corr</i>
DJF	11.2	12.6	31.1	30.6	17.5	16.2	51.7	46.7
MAM	16.1	16.5	41.4	45.5	24.2	21.4	51.7	52.6
JJA	10.0	8.1	16.4	15.6	3.6	3.2	-0.1	-1.7
SON	15.1	16.0	39.8	39.5	14.3	16.7	27.1	32.3

540
 541
 542
 543
 544
 545
 546
 547



548 **Table 5:** Summary of projected changes (°C) in monthly minimum of daily minimum temperature (TNn),
 549 monthly maximum of daily maximum temperature (TXx), and diurnal temperature range (DTR) for DJF,
 550 MAM, JJA, and SON during the 2071–2100 (2080s) relative to 1979–2008 (1990s) over the Mackenzie
 551 (MRB) and Saskatchewan (SRB) River basins.

	MRB						SRB					
	TXx		TNn		DTR		TXx		TNn		DTR	
	<i>raw</i>	<i>corr</i>										
DJF	4.5	4.4	9.4	9.4	-1.2	-1.2	2.8	2.7	9.3	9.3	-1.7	-1.9
MAM	3.4	3.3	7.3	7.4	-1.0	-1.4	3.2	3.0	5.9	6.1	-0.9	-1.1
JJA	6.2	6.2	6.1	6.1	0.1	0.1	7.2	7.2	6.7	6.8	0.4	0.4
SON	5.0	4.9	8.1	8.2	-0.7	-0.8	5.2	5.1	6.6	6.7	-0.4	-0.5

552

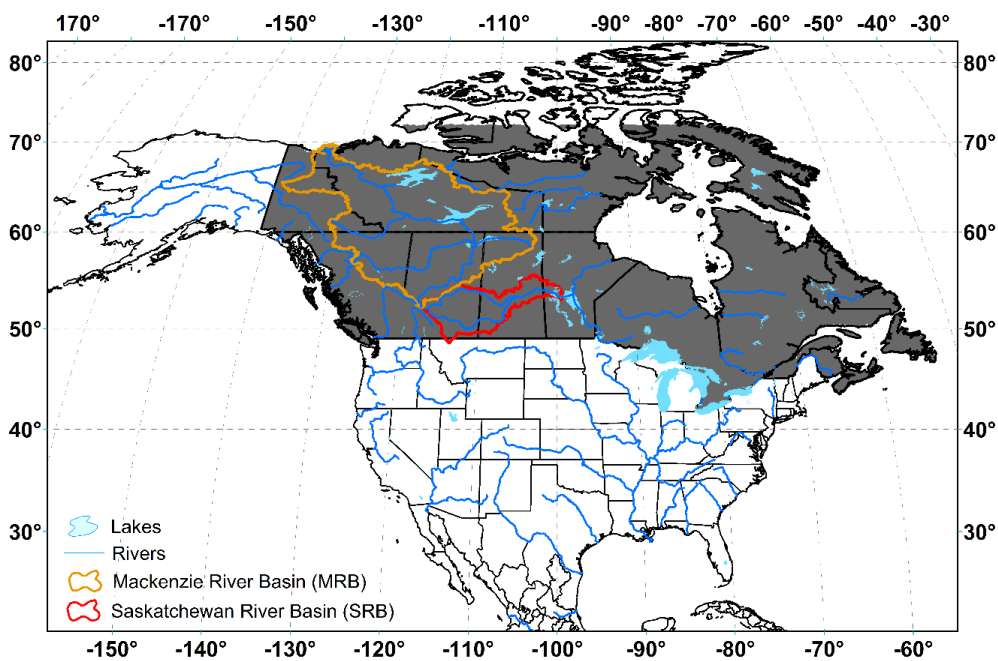
553

554

555



556 List of Figures



557

558 **Figure 1:** Study area (grey shading) ranges from longitude 50° W to 150° W and latitude 30° N to 72° N.

559 The orange and red polygons indicate the Mackenzie and Saskatchewan River basins, respectively, which
560 are testbeds for the Changing Cold Regions Network large-scale hydrological modelling strategy.

561

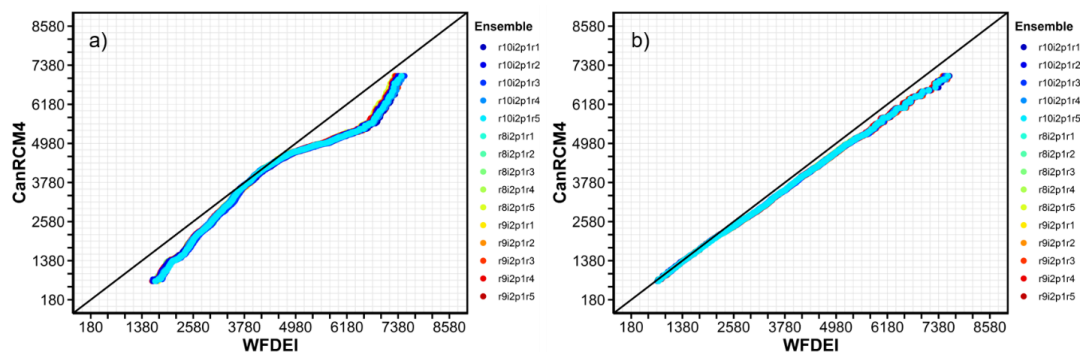
562

563

564

565

566



567

568 **Figure 2:** Quantile-quantile plots for days with >1 mm daily precipitation (R1mm) before (a) and after bias
569 correction (b). All grid points over the domain are used. The color scale indicates the fifteen ensemble
570 members utilized in this study.

571

572

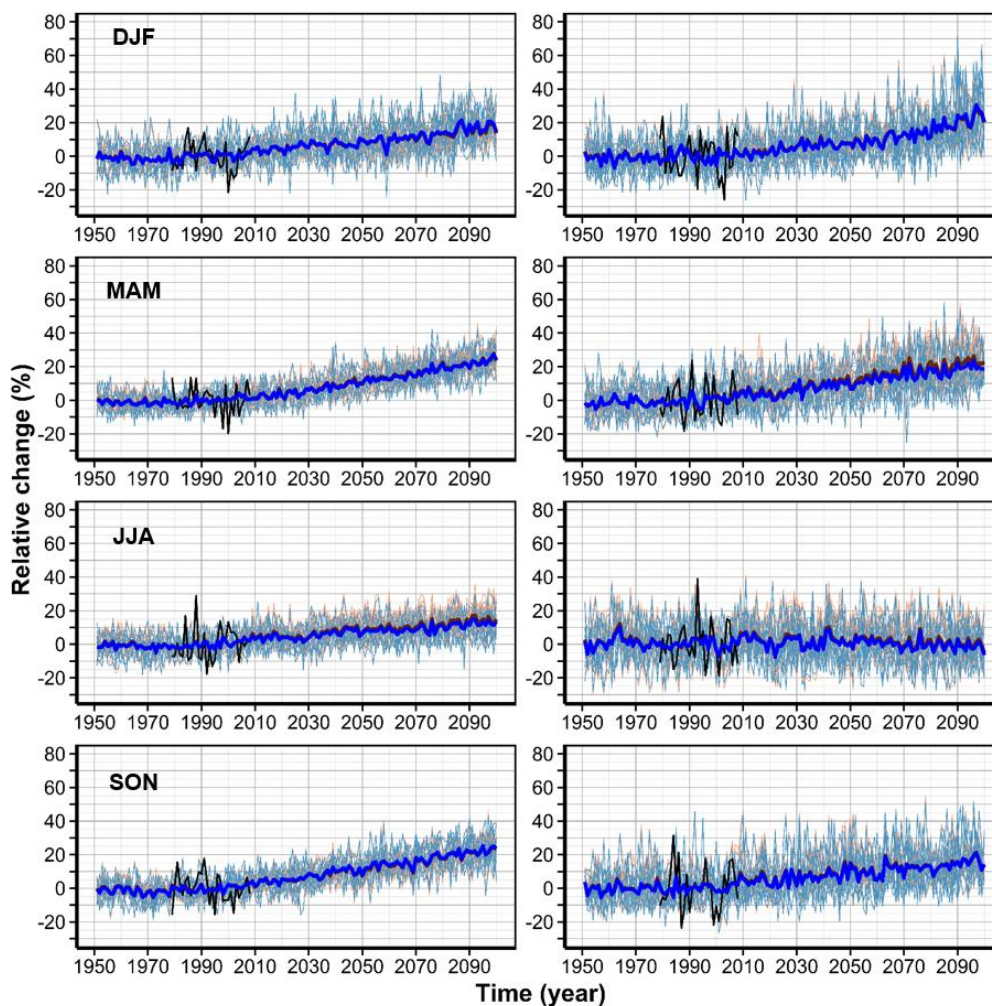
573

574

575

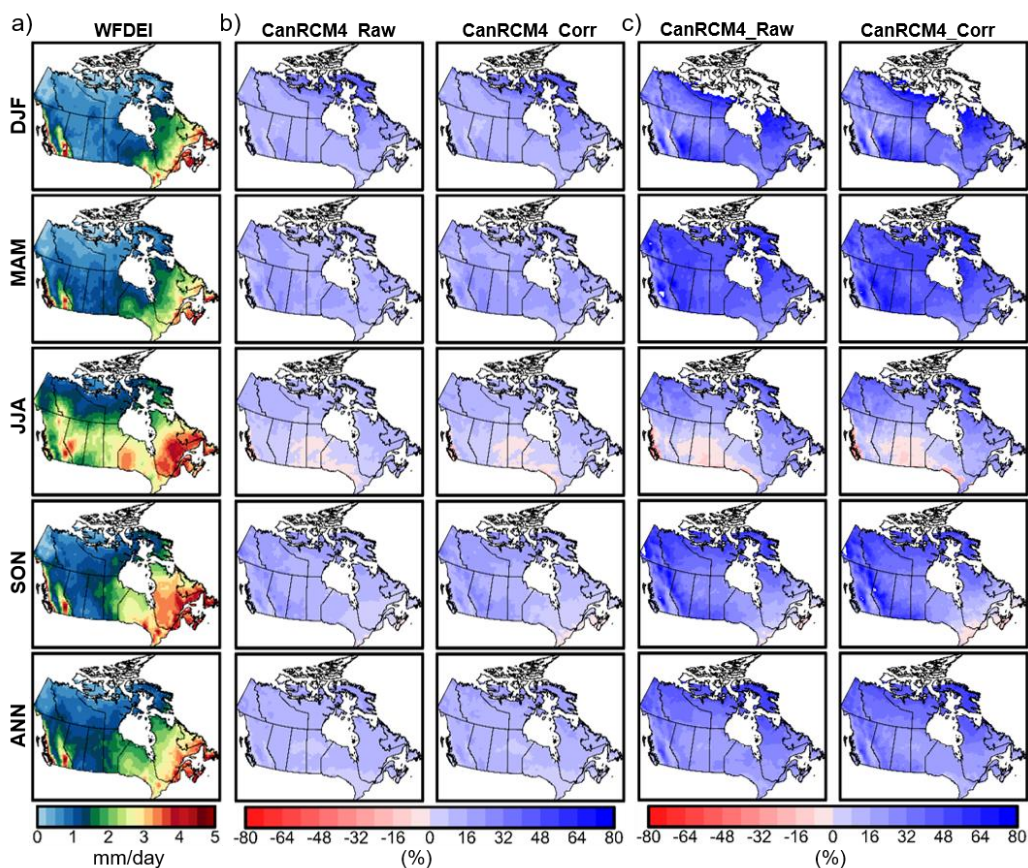
576

577



578

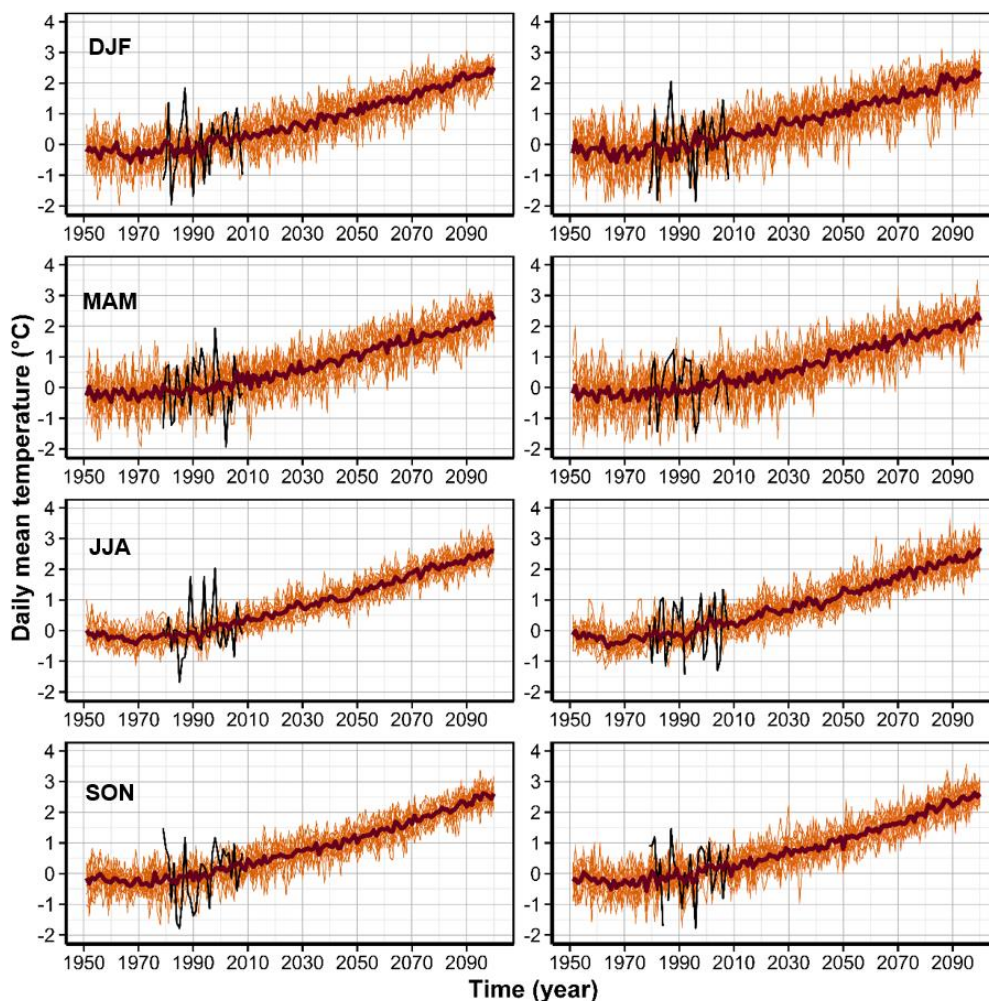
579 **Figure 3:** Temporal evolution (1950 – 2100) of basin-averaged mean daily precipitation for DJF, MAM, JJA,
580 and SON. The anomalies are displayed relative to the reference period 1979–2008. Solid lines indicate the
581 15-member ensemble mean while the shading denotes the spread across ensemble members. Time series
582 are shown for WFDEI (black), CanRCM4_Raw (red), and CanRCM4_Corr (blue) over the Mackenzie (left)
583 and Saskatchewan (right) River basins.



584

585 **Figure 4:** The multi-ensemble mean of climatologically averaged changes in daily mean precipitation (%)
586 for DJF, MAM, JJA, SON, and annual (ANN) during the 2021–2050 (b) and 2071–2100 (c) future periods
587 relative to 1979–2008. The spatial pattern of the observed WFDEI (a) product is also shown to aid in
588 understanding future changes in the spatial variation of precipitation. The results are displayed both for
589 the uncorrected (CanRCM4_Raw) and bias-corrected (CanRCM4_Corr) outputs.

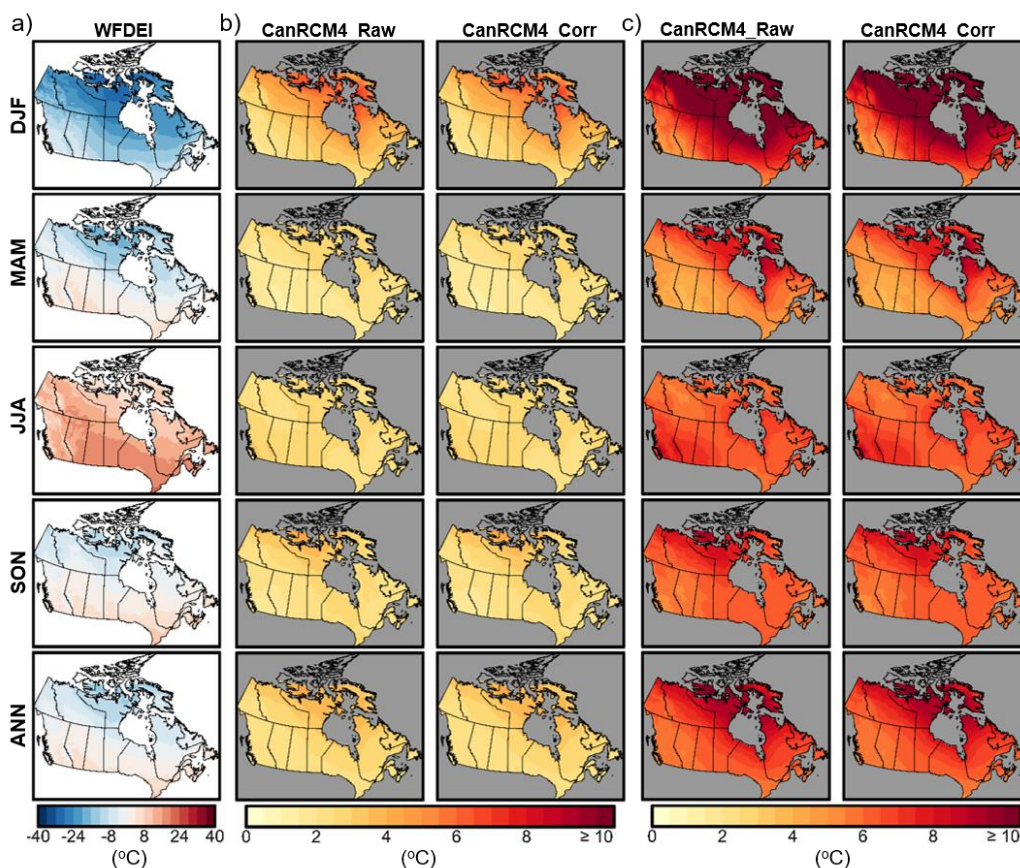
590



591

592 **Figure 5:** Temporal evolution (1950 – 2100) of basin-averaged daily mean temperature for DJF, MAM, JJA,
593 and SON. The anomalies are displayed relative to the reference period 1979–2008. Solid lines indicate the
594 15-member ensemble mean while the shading denotes the spread across ensemble members. Time series
595 are shown for WFDEI (black), CanRCM4_Raw (red), and CanRCM4_Corr (blue) over the Mackenzie (left)
596 and Saskatchewan (right) River basins.

597



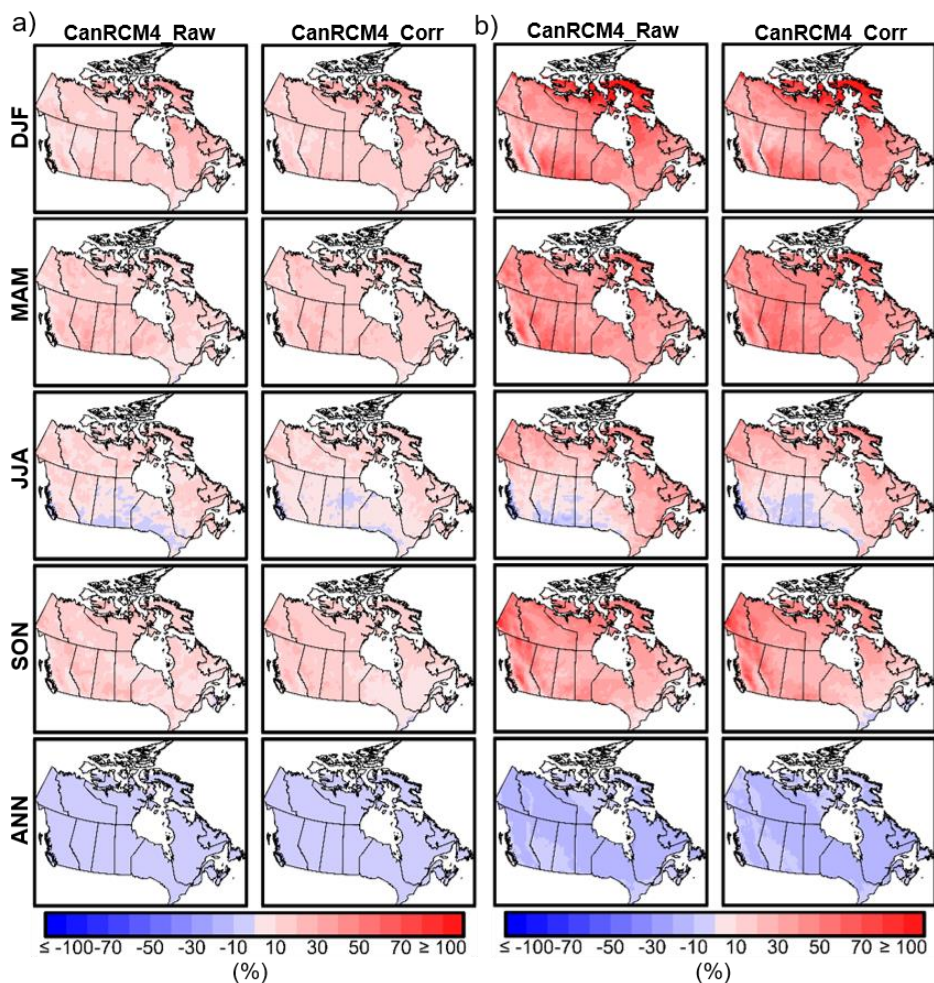
598

599 **Figure 6:** The ensemble mean of temporally averaged projected changes in daily mean temperature (°C)
600 for DJF, MAM, JJA, SON, and annual (ANN) during the 2021–2050 (b) and 2071–2100 (c) future periods as
601 differences from the historical period (1979–2008). The spatial pattern of the observed WFDEI (a) product
602 is also shown to aid in understanding future changes in the spatial structure of temperature. Other
603 information is the same as in Fig. 4.

604

605

606



607

608 **Figure 7:** The ensemble mean of temporally averaged projected changes in maximum 5-day precipitation

609 (RX5day) for DJF, MAM, JJA, SON, and annual (ANN) during the 2021–2050 (a) and 2071–2100 (b) future

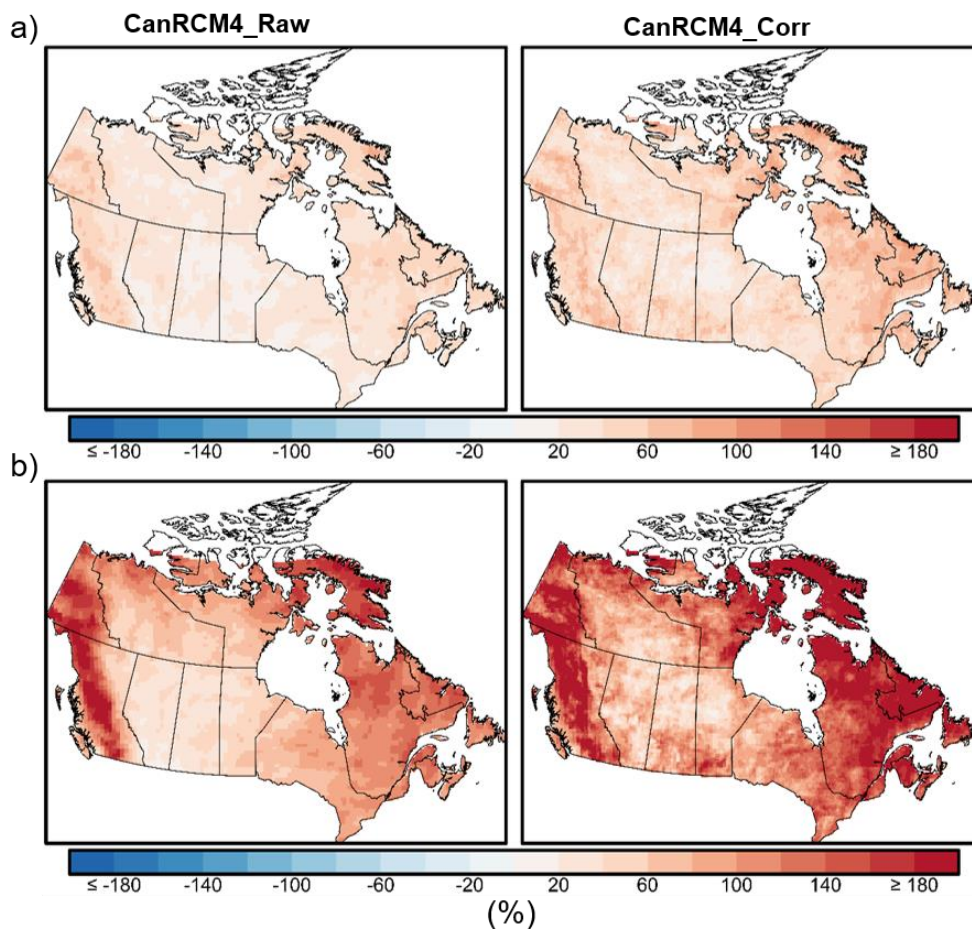
610 periods relative to 1979–2008. Other information is the same as in Fig. 4.

611

612

613

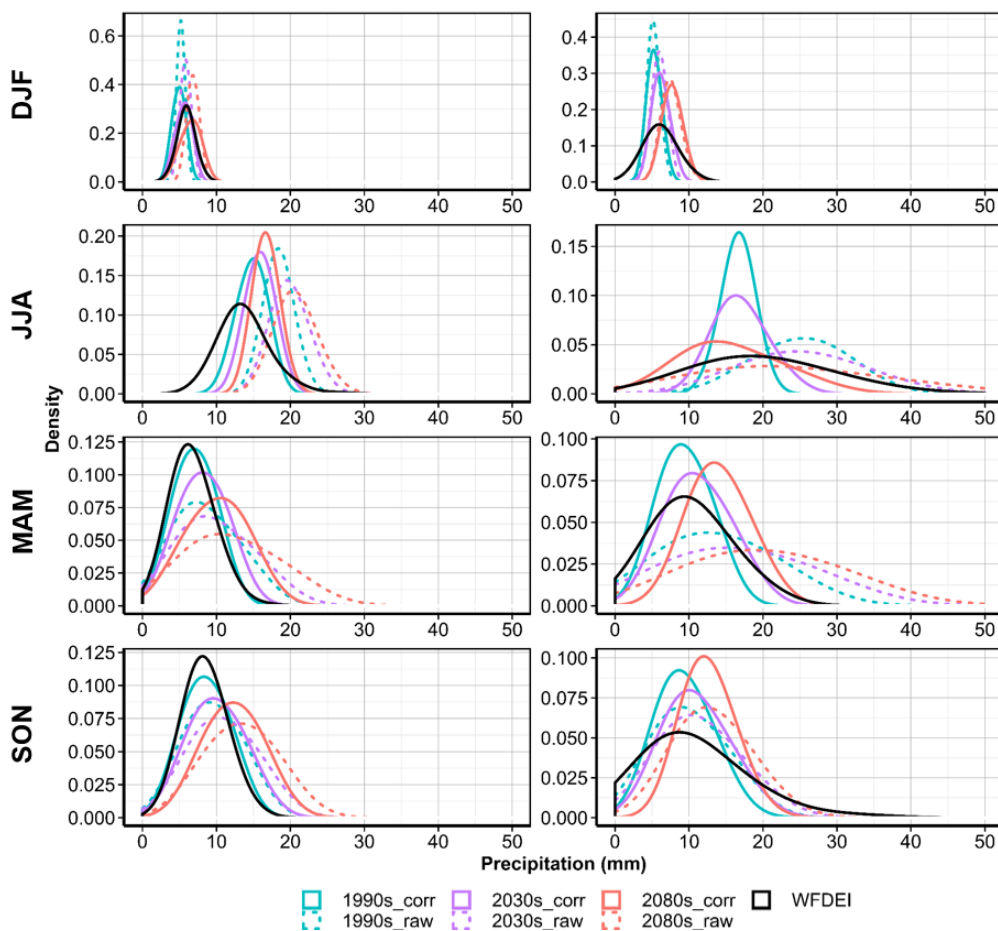
614



615

616 **Figure 8:** The ensemble mean of temporally averaged projected changes in extremely wet days (R99p)
617 during the 2021–2050 (a) and 2071–2100 (b) future periods relative to 1979–2008). Other information is
618 the same as in Fig. 4.

619



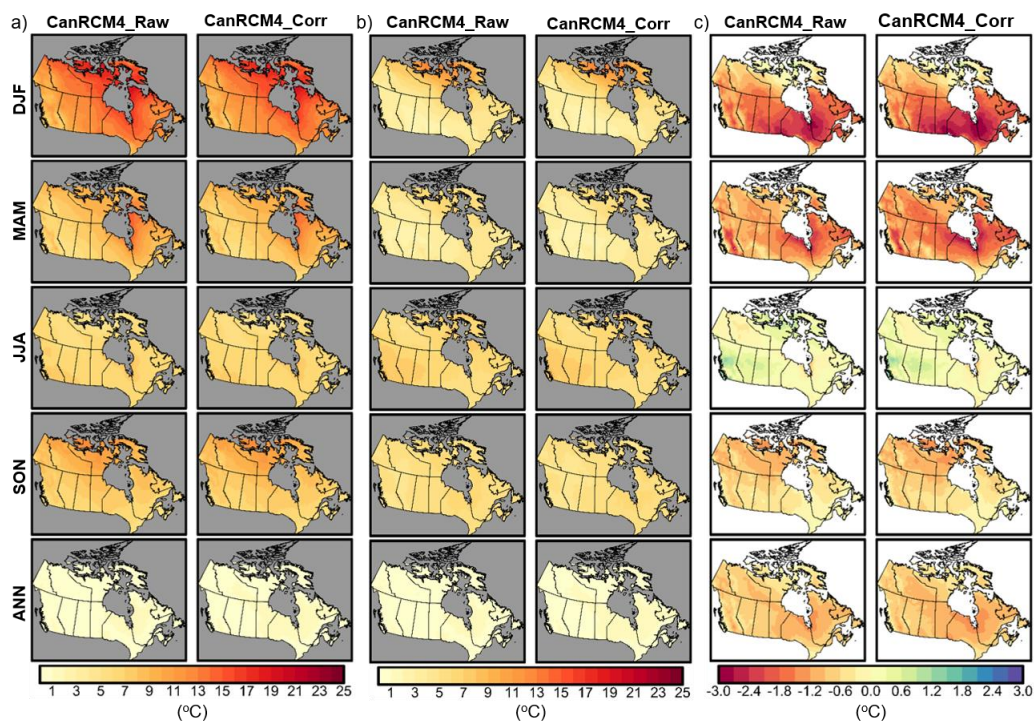
620

621 **Figure 9:** Probability distributions of seasonal maximum 1-day precipitation (RX1day) averaged over the
622 Mackenzie (left) and Saskatchewan (right) River basins for DJF, MAM, JJA, and SON, during the historical
623 (1979–2008) and two non-overlapping future periods (2021–2050 and 2071–2100). Results are shown for
624 WFDEI, and both the uncorrected (dotted line) and bias-corrected (solid line) CanRCM4 outputs.

625

626

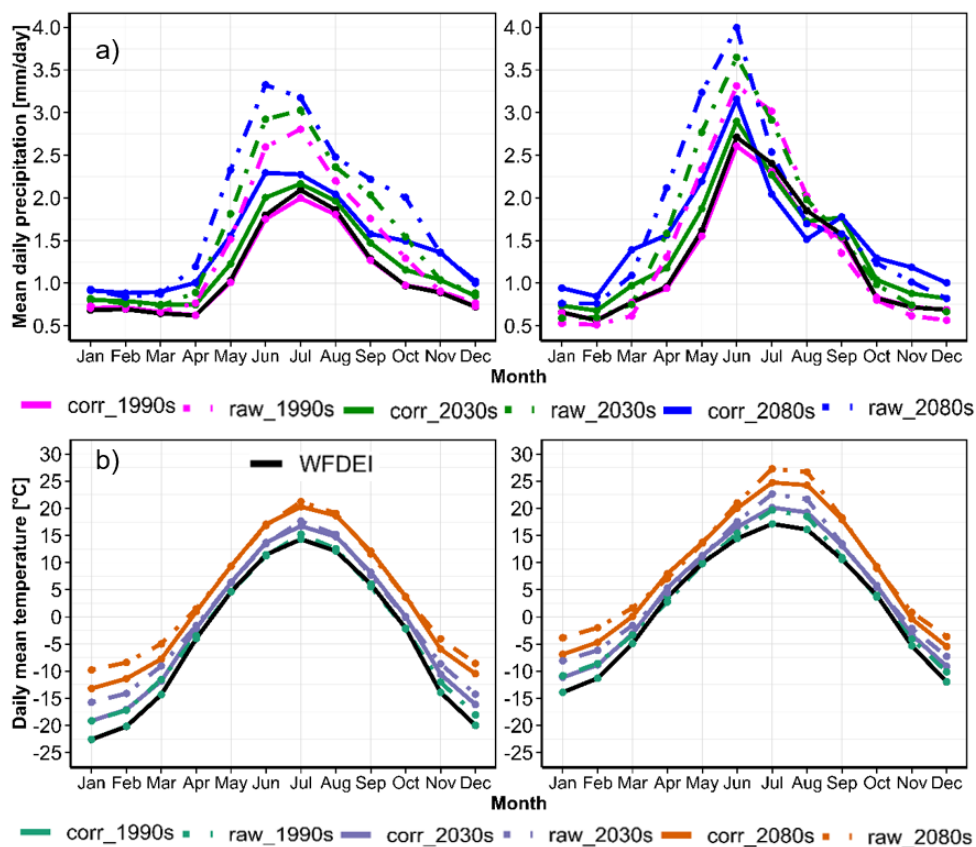
627



628

629 **Figure 10:** The ensemble mean of temporally averaged projected changes in monthly minimum of daily
630 minimum temperature (a), monthly maximum of daily maximum temperature (b), and diurnal
631 temperature range (c). Changes are calculated for the DJF, MAM, JJA, and SON seasons, as well as for the
632 whole year (ANN) during the 2071–2100 future period as differences from the historical period (1979–
633 2008). Other information is the same as in Fig. 4.

634



635

636 **Figure 11:** Seasonal cycle of mean daily precipitation (a) and daily mean temperature (b) for bias-corrected

637 CanRCM4 (solid) and raw CanRCM4 outputs (dotted) over the Mackenzie (left) and Saskatchewan (right)

638 River basins.

639

640

641

642

643

644

645



646 References

- 647 Allen, C. D., Macalady, A. K., Chenchouni, H., Bachelet, D., McDowell, N., Vennetier, M., Kitzberger,
648 T., Rigling, A., Breshears, D. D., and Hogg, E. T.: A global overview of drought and heat-induced tree
649 mortality reveals emerging climate change risks for forests, *Forest ecology and management*, 259, 660-
650 684, 2010.
- 651 Arnell, N.: *Climate change and drought, Options Méditerranéennes*, 2008.
- 652 Arnell, N. W.: *Climate change and global water resources, Global environmental change*, 9, S31-
653 S49, 1999.
- 654 Asong, Z. E., Khaliq, M. N., and Wheeler, H. S.: Regionalization of precipitation characteristics in
655 the Canadian Prairie Provinces using large-scale atmospheric covariates and geophysical attributes,
656 *Stochastic Environmental Research and Risk Assessment*, 29, 875-892, 10.1007/s00477-014-0918-z, 2015.
- 657 Asong, Z. E., Khaliq, M. N., and Wheeler, H. S.: Projected changes in precipitation and temperature
658 over the Canadian Prairie Provinces using the Generalized Linear Model statistical downscaling approach,
659 *Journal of Hydrology*, 539, 429-446, <http://dx.doi.org/10.1016/j.jhydrol.2016.05.044>, 2016b.
- 660 Asong, Z. E., Wheeler, H. S., Bonsal, B., Razavi, S., and Kurkute, S.: Historical drought patterns over
661 Canada and their teleconnections with large-scale climate signals, *Hydrol. Earth Syst. Sci.*, 22, 3105-3124,
662 10.5194/hess-22-3105-2018, 2018.
- 663 Bates, B., Kundzewicz, Z., and Wu, S.: *Climate change and water, Intergovernmental Panel on*
664 *Climate Change Secretariat*, 2008.
- 665 Beck, H. E., Vergopolan, N., Pan, M., Levizzani, V., van Dijk, A. I., Weedon, G. P., Brocca, L.,
666 Pappenberger, F., Huffman, G. J., and Wood, E. F.: Global-scale evaluation of 22 precipitation datasets
667 using gauge observations and hydrological modeling, *Hydrology and Earth System Sciences*, 21, 6201-
668 6217, 2017.
- 669 Behnke, R., Vavrus, S., Allstadt, A., Albright, T., Thogmartin, W. E., and Radeloff, V. C.: Evaluation
670 of downscaled, gridded climate data for the conterminous United States, *Ecological Applications*, 26,
671 1338-1351, doi:10.1002/15-1061, 2016.
- 672 Betts, R. A., Alfieri, L., Bradshaw, C., Caesar, J., Feyen, L., Friedlingstein, P., Gohar, L., Koutroulis,
673 A., Lewis, K., Morfopoulos, C., Papadimitriou, L., Richardson, K. J., Tsanis, I., and Wyser, K.: Changes in
674 climate extremes, fresh water availability and vulnerability to food insecurity projected at 1.5°C and
675 2°C global warming with a higher-resolution global climate model, *Philosophical Transactions of the*
676 *Royal Society A: Mathematical, Physical and Engineering Sciences*, 376, 20160452,
677 doi:10.1098/rsta.2016.0452, 2018.
- 678 Braganza, K., Karoly, D. J., and Arblaster, J. M.: Diurnal temperature range as an index of global
679 climate change during the twentieth century, *Geophysical Research Letters*, 31,
680 doi:10.1029/2004GL019998, 2004.
- 681 Burn, D. H.: Hydrologic effects of climatic change in west-central Canada, *Journal of Hydrology*,
682 160, 53-70, [https://doi.org/10.1016/0022-1694\(94\)90033-7](https://doi.org/10.1016/0022-1694(94)90033-7), 1994.
- 683 Burn, D. H., Whitfield, P. H., and Sharif, M.: Identification of changes in floods and flood regimes
684 in Canada using a peaks over threshold approach, *Hydrological Processes*, 30, 3303-3314,
685 10.1002/hyp.10861, 2016.
- 686 Burn, D. H., and Whitfield, P. H.: Changes in cold region flood regimes inferred from long-record
687 reference gauging stations, *Water Resources Research*, 53, 2643-2658, 10.1002/2016wr020108, 2017.
- 688 Cannon, A. J.: Multivariate Bias Correction of Climate Model Output: Matching Marginal
689 Distributions and Intervariable Dependence Structure, *Journal of Climate*, 29, 7045-7064, 10.1175/jcli-d-
690 15-0679.1, 2016.



691 Cannon, A. J.: Multivariate quantile mapping bias correction: an N-dimensional probability density
692 function transform for climate model simulations of multiple variables, *Climate Dynamics*, 50, 31-49,
693 10.1007/s00382-017-3580-6, 2018.

694 Chadburn, S. E., Burke, E. J., Essery, R. L. H., Boike, J., Langer, M., Heikenfeld, M., Cox, P. M., and
695 Friedlingstein, P.: Impact of model developments on present and future simulations of permafrost in a
696 global land-surface model, *The Cryosphere*, 9, 1505-1521, 10.5194/tc-9-1505-2015, 2015.

697 Coles, S., Bawa, J., Trenner, L., and Dorazio, P.: An introduction to statistical modeling of extreme
698 values, Springer, 2001.

699 Coopersmith, E. J., Minsker, B. S., and Sivapalan, M.: Patterns of regional hydroclimatic shifts: An
700 analysis of changing hydrologic regimes, *Water Resources Research*, 50, 1960-1983,
701 doi:10.1002/2012WR013320, 2014.

702 Das, T., Hidalgo, H. G., Pierce, D. W., Barnett, T. P., Dettinger, M. D., Cayan, D. R., Bonfils, C., Bala,
703 G., and Mirin, A.: Structure and Detectability of Trends in Hydrological Measures over the Western United
704 States, *Journal of Hydrometeorology*, 10, 871-892, 10.1175/2009jhm1095.1, 2009.

705 DeBeer, C. M., Wheeler, H. S., Carey, S. K., and Chun, K. P.: Recent climatic, cryospheric, and
706 hydrological changes over the interior of western Canada: a review and synthesis, *Hydrol. Earth Syst. Sci.*,
707 20, 1573-1598, 10.5194/hess-20-1573-2016, 2016.

708 Demaria, E. M. C., Roundy, J. K., Wi, S., and Palmer, R. N.: The Effects of Climate Change on
709 Seasonal Snowpack and the Hydrology of the Northeastern and Upper Midwest United States, *Journal of*
710 *Climate*, 29, 6527-6541, 10.1175/jcli-d-15-0632.1, 2016.

711 Dumanski, S., Pomeroy, J. W., and Westbrook, C. J.: Hydrological regime changes in a Canadian
712 Prairie basin, *Hydrological Processes*, 29, 3893-3904, doi:10.1002/hyp.10567, 2015.

713 Ehret, U., Zehe, E., Wulfmeyer, V., Warrach-Sagi, K., and Liebert, J.: HESS Opinions" Should we
714 apply bias correction to global and regional climate model data?", *Hydrology and Earth System Sciences*,
715 16, 3391-3404, 2012.

716 Erler, A. R., Peltier, W. R., and D'Orgeville, M.: Dynamically Downscaled High-Resolution
717 Hydroclimate Projections for Western Canada, *Journal of Climate*, 28, 423-450, 10.1175/jcli-d-14-00174.1,
718 2015.

719 Erler, A. R., and Peltier, W. R.: Projected Changes in Precipitation Extremes for Western Canada
720 based on High-Resolution Regional Climate Simulations, *Journal of Climate*, 29, 8841-8863, 10.1175/jcli-
721 d-15-0530.1, 2016.

722 Gleick, P. H.: Water, drought, climate change, and conflict in Syria, *Weather, Climate, and Society*,
723 6, 331-340, 2014.

724 Huppmann, D., Rogelj, J., Kriegler, E., Mundaca, L., Forster, P., Kobayashi, S., Séferian, R., and
725 Vilariño, M. V.: Scenario analysis notebooks for the IPCC Special Report on Global Warming of 1.5°C, in,
726 2018.

727 IPCC: Climate Change 2013: The Physical Science Basis. Contribution of Working Group I to the
728 Fifth Assessment Report of the Intergovernmental Panel on Climate Change, Cambridge University Press,
729 Cambridge, United Kingdom and New York, NY, USA, 1535 pp., 2013.

730 Islam, S. u., Déry, S. J., and Werner, A. T.: Future Climate Change Impacts on Snow and Water
731 Resources of the Fraser River Basin, British Columbia, *Journal of Hydrometeorology*, 18, 473-496,
732 10.1175/jhm-d-16-0012.1, 2017.

733 Ivanov, M. A., Luterbacher, J., and Kotlarski, S.: Climate Model Biases and Modification of the
734 Climate Change Signal by Intensity-Dependent Bias Correction, *Journal of Climate*, 31, 6591-6610,
735 10.1175/jcli-d-17-0765.1, 2018.

736 Jeong, D. I., Sushama, L., Diro, G. T., Khaliq, M. N., Beltrami, H., and Caya, D.: Projected changes
737 to high temperature events for Canada based on a regional climate model ensemble, *Climate Dynamics*,
738 46, 3163-3180, 10.1007/s00382-015-2759-y, 2016.



- 739 Johnson, F., and Sharma, A.: A nesting model for bias correction of variability at multiple time
740 scales in general circulation model precipitation simulations, *Water Resources Research*, 48,
741 doi:10.1029/2011WR010464, 2012.
- 742 Karl, T. R., Jones, P. D., Knight, R. W., Kukla, G., Plummer, N., Razuvayev, V., Gallo, K. P., Lindsey,
743 J., Charlson, R. J., and Peterson, T. C.: A new perspective on recent global warming: asymmetric trends of
744 daily maximum and minimum temperature, *Bulletin of the American Meteorological Society*, 74, 1007-
745 1024, 1993.
- 746 Karl, T. R., and Easterling, D. R.: Climate extremes: selected review and future research directions,
747 *Climatic change*, 42, 309-325, 1999.
- 748 Kharin, V. V., Zwiers, F. W., Zhang, X., and Hegerl, G. C.: Changes in Temperature and Precipitation
749 Extremes in the IPCC Ensemble of Global Coupled Model Simulations, *Journal of Climate*, 20, 1419-1444,
750 10.1175/jcli4066.1, 2007.
- 751 Kharin, V. V., Zwiers, F. W., Zhang, X., and Wehner, M.: Changes in temperature and precipitation
752 extremes in the CMIP5 ensemble, *Climatic Change*, 119, 345-357, 10.1007/s10584-013-0705-8, 2013.
- 753 Kundzewicz, Z. W., Krysanova, V., Dankers, R., Hirabayashi, Y., Kanae, S., Hattermann, F. F., Huang,
754 S., Milly, P. C. D., Stoffel, M., Driessen, P. P. J., Matczak, P., Quevauviller, P., and Schellnhuber, H. J.:
755 Differences in flood hazard projections in Europe – their causes and consequences for decision making,
756 *Hydrological Sciences Journal*, 62, 1-14, 10.1080/02626667.2016.1241398, 2017.
- 757 Laprise, R.: Regional climate modelling, *Journal of Computational Physics*, 227, 3641-3666, 2008.
- 758 Lewis, S. C., and Karoly, D. J.: Evaluation of Historical Diurnal Temperature Range Trends in CMIP5
759 Models, *Journal of Climate*, 26, 9077-9089, 10.1175/jcli-d-13-00032.1, 2013.
- 760 Li, Y., Ye, W., Wang, M., and Yan, X.: Climate change and drought: a risk assessment of crop-yield
761 impacts, *Climate research*, 39, 31-46, 2009.
- 762 Mahfouf, J. F., Brasnett, B., and Gagnon, S.: A Canadian precipitation analysis (CaPA) project:
763 Description and preliminary results, *Atmosphere-Ocean*, 45, 1-17, 10.3137/ao.v45i0101, 2007.
- 764 Mann, M. E., and Gleick, P. H.: Climate change and California drought in the 21st century,
765 *Proceedings of the National Academy of Sciences*, 112, 3858-3859, 2015.
- 766 Maraun, D., Wetterhall, F., Ireson, A. M., Chandler, R. E., Kendon, E. J., Widmann, M., Brienen, S.,
767 Rust, H. W., Sauter, T., Themeßl, M., Venema, V. K. C., Chun, K. P., Goodess, C. M., Jones, R. G., Onof, C.,
768 Vrac, M., and Thiele-Eich, I.: Precipitation downscaling under climate change: Recent developments to
769 bridge the gap between dynamical models and the end user, *Reviews of Geophysics*, 48,
770 doi:10.1029/2009RG000314, 2010.
- 771 Maraun, D., Shepherd, T. G., Widmann, M., Zappa, G., Walton, D., Gutiérrez, J. M., Hagemann, S.,
772 Richter, I., Soares, P. M. M., Hall, A., and Mearns, L. O.: Towards process-informed bias correction of
773 climate change simulations, *Nature Climate Change*, 7, 764, 10.1038/nclimate3418, 2017.
- 774 Mesinger, F., DiMego, G., Kalnay, E., Mitchell, K., Shafran, P. C., Ebisuzaki, W., Jović, D., Woollen,
775 J., Rogers, E., and Berbery, E. H.: North American regional reanalysis, *Bulletin of the American
776 Meteorological Society*, 87, 343-360, 2006.
- 777 Monette, A., Sushama, L., Khaliq, M. N., Laprise, R., and Roy, R.: Projected changes to precipitation
778 extremes for northeast Canadian watersheds using a multi-RCM ensemble, *Journal of Geophysical
779 Research: Atmospheres*, 117, 10.1029/2012jd017543, 2012.
- 780 Musselman, K. N., Lehner, F., Ikeda, K., Clark, M. P., Prein, A. F., Liu, C., Barlage, M., and
781 Rasmussen, R.: Projected increases and shifts in rain-on-snow flood risk over western North America,
782 *Nature Climate Change*, 8, 808-812, 10.1038/s41558-018-0236-4, 2018.
- 783 Park, H., Yoshikawa, Y., Oshima, K., Kim, Y., Ngo-Duc, T., Kimball, J. S., and Yang, D.: Quantification
784 of Warming Climate-Induced Changes in Terrestrial Arctic River Ice Thickness and Phenology, *Journal of
785 Climate*, 29, 1733-1754, 10.1175/jcli-d-15-0569.1, 2016.



- 786 Pederson, G. T., Gray, S. T., Ault, T., Marsh, W., Fagre, D. B., Bunn, A. G., Woodhouse, C. A., and
787 Graumlich, L. J.: Climatic Controls on the Snowmelt Hydrology of the Northern Rocky Mountains, *Journal*
788 *of Climate*, 24, 1666-1687, 10.1175/2010jcli3729.1, 2011.
- 789 Pomeroy, J. W., Fang, X., and Marks, D. G.: The cold rain-on-snow event of June 2013 in the
790 Canadian Rockies — characteristics and diagnosis, *Hydrological Processes*, 30, 2899-2914,
791 10.1002/hyp.10905, 2016.
- 792 Sapiano, M. R. P., and Arkin, P. A.: An Intercomparison and Validation of High-Resolution Satellite
793 Precipitation Estimates with 3-Hourly Gauge Data, *Journal of Hydrometeorology*, 10, 149-166,
794 10.1175/2008jhm1052.1, 2009.
- 795 Scinocca, J. F., Kharin, V. V., Jiao, Y., Qian, M. W., Lazare, M., Solheim, L., Flato, G. M., Biner, S.,
796 Desgagne, M., and Dugas, B.: Coordinated Global and Regional Climate Modeling, *Journal of Climate*, 29,
797 17-35, 10.1175/jcli-d-15-0161.1, 2016.
- 798 Sheffield, J., Goteti, G., and Wood, E. F.: Development of a 50-year high-resolution global dataset
799 of meteorological forcings for land surface modeling, *Journal of Climate*, 19, 3088-3111, 2006.
- 800 Sillmann, J., Kharin, V., Zwiers, F., Zhang, X., and Bronaugh, D.: Climate extremes indices in the
801 CMIP5 multimodel ensemble: Part 2. Future climate projections, *Journal of Geophysical Research:*
802 *Atmospheres*, 118, 2473-2493, 2013a.
- 803 Sillmann, J., Kharin, V. V., Zhang, X., Zwiers, F. W., and Bronaugh, D.: Climate extremes indices in
804 the CMIP5 multimodel ensemble: Part 1. Model evaluation in the present climate, *Journal of Geophysical*
805 *Research: Atmospheres*, 118, 1716-1733, doi:10.1002/jgrd.50203, 2013b.
- 806 Stocker, T. F., Qin, D., Plattner, G.-K., Alexander, L. V., Allen, S. K., Bindoff, N. L., Bréon, F.-M.,
807 Church, J. A., Cubasch, U., Emori, S., Forster, P., Friedlingstein, P., Gillett, N., Gregory, J. M., Hartmann, D.
808 L., Jansen, E., Kirtman, B., Knutti, R., Krishna Kumar, K., Lemke, P., Marotzke, J., Masson-Delmotte, V.,
809 Meehl, G. A., Mokhov, I. I., Piao, S., Ramaswamy, V., Randall, D., Rhein, M., Rojas, M., Sabine, C., Shindell,
810 D., Talley, L. D., Vaughan, D. G., and Xie, S.-P.: Technical Summary, in: *Climate Change 2013: The Physical*
811 *Science Basis. Contribution of Working Group I to the Fifth Assessment Report of the Intergovernmental*
812 *Panel on Climate Change*, edited by: Stocker, T. F., Qin, D., Plattner, G.-K., Tignor, M., Allen, S. K., Boschung,
813 J., Nauels, A., Xia, Y., Bex, V., and Midgley, P. M., Cambridge University Press, Cambridge, United Kingdom
814 and New York, NY, USA, 33–115, 2013.
- 815 Thorne, P. W., Donat, M. G., Dunn, R. J. H., Williams, C. N., Alexander, L. V., Caesar, J., Durre, I.,
816 Harris, I., Hausfather, Z., Jones, P. D., Menne, M. J., Rohde, R., Vose, R. S., Davy, R., Klein-Tank, A. M. G.,
817 Lawrimore, J. H., Peterson, T. C., and Rennie, J. J.: Reassessing changes in diurnal temperature range:
818 Intercomparison and evaluation of existing global data set estimates, *Journal of Geophysical Research:*
819 *Atmospheres*, 121, 5138-5158, doi:10.1002/2015JD024584, 2016.
- 820 Vincent, L. A., Zhang, X., Brown, R. D., Feng, Y., Mekis, E., Milewska, E. J., Wan, H., and Wang, X.
821 L.: Observed Trends in Canada's Climate and Influence of Low-Frequency Variability Modes, *Journal of*
822 *Climate*, 28, 4545-4560, 10.1175/jcli-d-14-00697.1, 2015.
- 823 Volosciuk, C., Maraun, D., Vrac, M., and Widmann, M.: A combined statistical bias correction and
824 stochastic downscaling method for precipitation, *Hydrol. Earth Syst. Sci.*, 21, 1693-1719, 10.5194/hess-
825 21-1693-2017, 2017.
- 826 Wang, X., Huang, G., Liu, J., Li, Z., and Zhao, S.: Ensemble Projections of Regional Climatic Changes
827 over Ontario, Canada, *Journal of Climate*, 28, 7327-7346, 10.1175/jcli-d-15-0185.1, 2015.
- 828 Weedon, G. P., Balsamo, G., Bellouin, N., Gomes, S., Best, M. J., and Viterbo, P.: The WFDEI
829 meteorological forcing data set: WATCH Forcing Data methodology applied to ERA-Interim reanalysis
830 data, *Water Resources Research*, 50, 7505-7514, doi:10.1002/2014WR015638, 2014.
- 831 Wilby, R. L., and Dessai, S.: Robust adaptation to climate change, *Weather*, 65, 180-185,
832 10.1002/wea.543, 2010.



- 833 Wilby, R. L.: Climate Change in Practice: Topics for Discussion with Group Exercises, Cambridge
834 University Press, Cambridge, 2017.
- 835 Willkofer, F., Schmid, F.-J., Komischke, H., Korck, J., Braun, M., and Ludwig, R.: The impact of bias
836 correcting regional climate model results on hydrological indicators for Bavarian catchments, *Journal of*
837 *Hydrology: Regional Studies*, 19, 25-41, <https://doi.org/10.1016/j.ejrh.2018.06.010>, 2018.
- 838 Wong, J. S., Razavi, S., Bonsal, B. R., Wheater, H. S., and Asong, Z. E.: Inter-comparison of daily
839 precipitation products for large-scale hydro-climatic applications over Canada, *Hydrol. Earth Syst. Sci.*, 21,
840 2163-2185, 10.5194/hess-21-2163-2017, 2017.
- 841 Woo, M.-k., Lewkowitz, A. G., and Rouse, W. R.: Response of the Canadian permafrost
842 environment to climatic change, *Physical geography*, 13, 287-317, 1992.
- 843 Woo, M.-K., and Pomeroy, J.: *Snow and Runoff: Processes, Sensitivity and Vulnerability*, in:
844 *Changing Cold Environments*, John Wiley & Sons, Ltd, 105-125, 2011.
- 845 Wood, A. W., Leung, L. R., Sridhar, V., and Lettenmaier, D.: Hydrologic implications of dynamical
846 and statistical approaches to downscaling climate model outputs, *Climatic change*, 62, 189-216, 2004.
- 847 Yeh, K.-S., Côté, J., Gravel, S., Méthot, A., Patoine, A., Roch, M., and Staniforth, A.: The CMC-MRB
848 Global Environmental Multiscale (GEM) Model. Part III: Nonhydrostatic Formulation, *Monthly Weather*
849 *Review*, 130, 339-356, 10.1175/1520-0493(2002)130<0339:tcmgem>2.0.co;2, 2002.
- 850 You, Q., Wang, D., Jiang, Z., and Kang, S.: Diurnal temperature range in CMIP5 models and
851 observations on the Tibetan Plateau, *Quarterly Journal of the Royal Meteorological Society*, 143, 1978-
852 1989, doi:10.1002/qj.3057, 2017.
- 853 Zhang, X., Alexander, L., Hegerl, G. C., Jones, P., Tank, A. K., Peterson, T. C., Trewin, B., and Zwiers,
854 F. W.: Indices for monitoring changes in extremes based on daily temperature and precipitation data,
855 *Wiley Interdisciplinary Reviews: Climate Change*, 2, 851-870, doi:10.1002/wcc.147, 2011.
- 856